
Predicting Adversarial Examples with High Confidence

Angus Galloway^{1,2} Graham W. Taylor^{1,2,3} Medhat Moussa¹

Abstract

It has been suggested that *adversarial examples* cause deep learning models to make incorrect predictions with high confidence. In this work, we take the opposite stance: an overly confident *model* is more likely to be vulnerable to adversarial examples. This work is one of the most proactive approaches taken to date, as we link robustness with *non-calibrated* model confidence on noisy images, providing a data-augmentation-free path forward. The *adversarial examples phenomenon* is most easily explained by the trend of increasing non-regularized model capacity, while the diversity and number of samples in common datasets has remained flat. Test accuracy has incorrectly been associated with true *generalization performance*, ignoring that training and test splits are often extremely similar in terms of the overall representation space. The transferability property of adversarial examples was previously used as evidence against overfitting arguments, a perceived random effect, but overfitting is not always random.

1. Introduction

Practically obtainable datasets are inherently sparse in high-dimensions. This is true for image classification tasks like the CIFAR-10 and ImageNet datasets, on which deep neural networks have achieved very low test error. The *adversarial examples* phenomenon was an observation that these same state-of-the-art deep learning models are easily fooled by images that are objectively very similar to the naturally occurring data on which they were trained (Szegedy et al., 2014). The effect implies two seemingly contradictory statements, which Jo & Bengio (2017) and Dube (2018) summarize well: on one hand, deep neural networks generalize extremely well to a held-out test set, yet any randomly

selected correctly classified image is arbitrarily close to a misclassified one.

Several hypotheses have been proposed regarding this phenomenon, such as the idea that adversarial examples occupy small low-probability “pockets” in the manifold, yet are dense, similar to rational numbers on the real line (Szegedy et al., 2014). However, it would be unusual that neural networks are learning a decision boundary anything like the distribution of rational and irrational numbers on the number line. Furthermore, an effect where images initialized with random noise are classified with very high confidence (Nguyen et al., 2015) suggests that there exists at least one class of “non-examples” that do not occur in low-probability pockets, but can be found almost everywhere in the representation space not spanned by the sparse training data.

The linearity hypothesis of Goodfellow et al. (2015) suggests that for a model parameterized by weights w with an average magnitude of m , and input $x \in \mathbb{R}^n$, one need only perturb x by a vector of small constants ϵ aligned in the direction of w to induce a swing in activation of ϵmn . They argue that ϵ shrinks with increasing n ; however Tanay & Griffin (2016) remind us that the magnitude of the activations also grows linearly with n . They demonstrate that linear behaviour alone is insufficient to cause adversarial examples, and our experiments confirm this.

Non-examples occupy space within the representation ability of our models that has yet to be explored. In high dimensions, these areas will never be explored, therefore it is logical to attempt to use strong regularization to reduce representation ability such that we minimize the space away from the training data sub-manifolds.

We show that not all methods of minimizing the unexplored space are equivalent. Experiments on the synthetic spheres dataset from Gilmer et al. (2018) suggests that using low-precision representations appears to confer additional pose-invariance characteristics upon a model, with the added benefit of compression and easing model deployment on general purpose hardware. In this regard, we expand on the work of Galloway et al. (2018) that compared the robustness of full-precision and binarized models, finding that the lower precision variant was equally or more robust to a variety of attacks.

¹School of Engineering, University of Guelph, Canada ²Vector Institute for Artificial Intelligence, Canada ³Canadian Institute for Advanced Research. Correspondence to: Angus Galloway <gallowaa@uoguelph.ca>.

One of our main contributions is a comparison of regularization effects of arbitrarily low-precision internal representations against traditional methods of regularizing a model, such as weight decay. We then explore a fundamental trade-off between preserving sensitivity to valid natural image classes, and reducing total unexplored space. To the best of our knowledge, we are also the first to defend against *fooling images* (Nguyen et al., 2015), also known as “rubbish class” examples, without using RBF networks which do not generalize well (Goodfellow et al., 2015).

2. Background

Regularization was investigated as a potential solution to the adversarial problem as early as in Szegedy et al. (2014), but was discarded in subsequent work (Goodfellow et al., 2015) after modest amounts of L_1 weight decay did not completely resolve the problem. We additionally suspect the transferability property: that adversarial examples generated on one architecture (e.g. ResNets) are likely to be misclassified by others trained independently (e.g. VGG, Inception), was seen as evidence *against* overfitting. As overfitting is traditionally viewed as a *random* effect that leads to poor generalization on the test set, researchers falsely concluded that adversarial examples and overfitting are unrelated. We maintain that training over-parameterized models on the same datasets, using the same optimization procedure, is sufficient to cause non-random overfitting.

Additional work similar to regularization includes Fawzi et al. (2015), who found that training on random noise also was not beneficial. Eventually, the suggestions of Szegedy et al. (2014) were implemented by Cisse et al. (2017), in which the Lipschitz constant of various layers is constrained to be ≤ 1 . The idea was to prevent instabilities from propagating through the network, but in practice resulted in modest gains beyond those conferred by adversarial training data-augmentation approaches. Additionally, Cisse et al. (2017) did not conduct an in-depth analysis against traditional regularization techniques like weight decay, beyond mentioning that they used some weight decay in their experiments. As we show, the “state-of-the-art” architectures they used are very fragile to strong weight decay, which likely discouraged them and others from exploring this further.

Gu & Rigazio (2015) proposed using “deep contractive networks”, which they argued makes the model more flat near the training data by introducing a smoothness penalty inspired by a contractive autoencoder (CAE). The main idea was that making the model’s decision boundary more flat near the training data manifold should maximize the L_2 distortion required to cause misclassification. They also noticed that denoising autoencoders are able to recover 90% of adversarial errors by reconstructing examples as a pre-processing step. Nonetheless, when they attempted to stack

the autoencoder with a (poorly regularized) classifier, the overall model was easily defeated in an end-to-end attack. Ultimately, while we do agree that smoothness is desirable near the training data to a limited extent since an n -sphere maximizes distance to the surface for a fixed volume sub-manifold, Gu & Rigazio do not address the behaviour of their model globally, *away* from the training data. This likely leaves it vulnerable to the gradient ascent “fooling images” attack (Nguyen et al., 2015). Additionally, their results are reported in terms of the L_2 input distortion that causes a 100% misclassification rate, which is difficult to compare with other literature on neural network defenses.

Bau et al. (2017) propose a framework for automatically quantifying disentangled representations in deep CNNs by network dissection. Although they do not explicitly focus on robustness to adversarial perturbations, their work is complementary to ours in that they observe a significant degree of variability in the interpretability of different models that all obtain very similar “generalization” performance on the test set.

As of ICLR 2018, the only non-certified defense that has lived up to claims made for a white-box threat model, after a recent informal investigation by Athalye et al. (2018), is that of Madry et al. (2018). Although the work of Athalye et al. (2018) has not yet undergone official peer review, we believe their methodology to be sound and in keeping with techniques that defeated similar previously published defenses with *gradient masking* tendencies (Papernot et al., 2015; Gu & Rigazio, 2015). Many of the defeated ICLR 2018 defenses showed signs of gradient masking, or tested on attacks that were too weak (Dhillon et al., 2018; Buckman et al., 2018; Guo et al., 2018; Samangouei et al., 2018; Song et al., 2018; Xie et al., 2018). Defense strategies that rely solely on gradient masking do not improve the richness of features learned, or affect the underlying geometry of the decision boundary in a meaningful way, which ultimately determines real-world robustness in the practical black-box setting. The white-box model, however, is convenient to study as it is strictly more difficult to defend against than black-box. Therefore, if a model is robust against the former, it also is against the latter.

Expectation over Transformation (EOT) is a sampling technique that overcomes defenses relying on stochasticity by attacking them end-to-end after averaging gradients over several (e.g. 10 or more) forward passes, before taking a backward step. It has been shown to create reliable adversarial examples against a variety of random viewpoint transformations, such as over changes in scale and rotation in 2 or 3D (Athalye et al., 2017). It is conceivable that variants of the same attack can be used against even the most creative defenses, such as Defense-GAN, where the non-trust worthy input image is first encoded into a latent space, substituted

with its nearest neighbor, and then classified (Samangouei et al., 2018). The attack exploits the concurrently demonstrated notion that adversarial examples can exist directly on the data manifold, for a synthetic concentric spheres data set (Gilmer et al., 2018).

It is also highly plausible that non-differentiable input transformations blocking gradient flow can confidently be back-propagated through using the same straight through gradient estimator (STE) commonly used to train binarized and low-precision neural networks to high accuracy (Bengio et al., 2013; Courbariaux & Bengio, 2016; Zhou et al., 2016). This is essentially the “Backward Pass Differentiable Approximation” used to bypass defenses that destroy gradient signal in Athalye et al. (2018).

3. The Madry et al. (2018) Defense

The Madry et al. (2018) defense uses projected gradient descent (PGD) (Kurakin et al., 2017) with a random initialization to defend against perturbations $\mathcal{S} \subseteq \mathbb{R}^d$ allowed under the threat model. More formally, it consists of a min-max optimization game defined by (1). The inner maximization consists of adding a random (e.g. uniform) L_p bounded perturbation $\delta \in \mathcal{S}$ to the input x , and then taking several steps in the direction of the gradient that maximizes the training loss J with respect to x . For each step in the inner maximization loop, the sign of the gradient is usually scaled by a constant ϵ and accumulated in x . The outer minimization is a normal update to model parameters θ by stochastic gradient descent on the loss obtained with this new batch of adversarial examples.

$$\min_{\theta} \left(\mathbb{E}_{(x,y) \sim \mathcal{D}} \left[\max_{\delta \in \mathcal{S}} J(\theta, x + \delta, y) \right] \right) \quad (1)$$

Their particular claim of robustness considers perturbations up to $\epsilon = 0.3$ and $8/255$ under the L_∞ norm for the MNIST and CIFAR-10 data sets respectively. The L_∞ norm is a reasonable choice since it strictly maximizes all preceding L_p -norms (e.g. L_1, L_2), which explains why they see favourable performance against L_2 bounded attacks in their Figure 6, despite never training with an L_2 bounded adversary. We can derive an upper limit for an L_∞ trained model in terms of L_2 robustness on an n dimensional data set given that $\|x\|_2 \leq \sqrt{n}\|x\|_\infty$. This implies a theoretical upper L_2 limit of 8.4 for MNIST, and $443/255$ for CIFAR-10. Interestingly, both MNIST and CIFAR-10 models in Figure 6 of the Madry et al. (2018) paper use roughly 10% of this theoretical limit, a quantity determined by picking an accuracy level on the L_∞ plot and mapping it to ϵ where the same value occurs on the L_2 plot. This could be explained by the choice of sampling the initial random perturbation from a uniform distribution, which will only have a few values that saturate the limits of $\pm\epsilon$. In any case, the initial

random perturbation has proven to be critically important for increasing the diversity of examples trained against during training, as opposed to the original deterministic fast gradient method (Goodfellow et al., 2015).

Despite the success of data-augmentation approaches to date, we share the opinion of Jo & Bengio (2017) regarding their long-term suitability, as it is hard to guarantee that a *different* attack will not be successful against the particular adversary used during training. Additionally, the choice of threat model assumed in data-augmentation based defenses is often arbitrary, and performance has been found to rapidly decay for perturbations just slightly beyond that seen by the model in training (Kurakin et al., 2017; Madry et al., 2018).

4. Experiments on the Madry Defense

We believe it is imperative that the community move away from solely data-augmentation based approaches as a defense mechanism. For example, the min-max game-theoretic nature of (1) assumes an attacker is playing the same game. This is confirmed by our experiments against the Madry et al. (2018) defense, as we find at least one *zero* and *first-order* “blindspot”, where behaviour is demonstrably worse than un-defended or well regularized model.

4.1. Constant Pixel Intensity Attack

In Figure 1, a gradient-free, or “zero-order”, attack is deployed against the state-of-the-art models provided online by Madry et al. (2018) that were secured with PGD. The attack is trivial in nature, and simply involves adding a constant offset (positive or negative) to the image, and then clipping to the valid pixel range. There are legitimate concerns about this weakness, and many reasons to expect the background colour to differ in a real world machine vision application. Humans have no trouble reading digits or classifying images registered against a clean, uniform background, even when the difference between the pixel intensities in the foreground and background is small.

The attack was motivated by an analysis of the learned convolutional kernels in Madry et al. (2018) (in particular, Figure 9 in the paper, and the surrounding discussion in Appendix E), in which they mention that the first layer implements a learned thresholding filter. All but *three* of thirty-two kernels in the first layer of the three-layer CNN were approximately *zero*. Among the three kernels that were not all zeros, each had only *one* element that was non-zero. The function of the *entire* first layer for the PGD trained model is to scale and threshold. The reason this could be an optimal strategy against a PGD adversary is that, in combination with learned biases, perturbations up to ϵ_{\max} are forced to the non-linear region of the ReLU activations.

Both of the independently trained “secret” and “public”

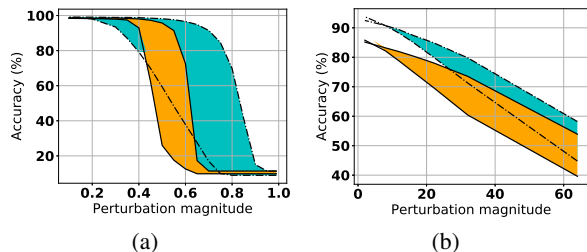


Figure 1. Attacking the state-of-the-art “secret” model from the black-box (a) MNIST and (b) CIFAR-10 robustness challenges hosted by Madry et al. (2018)¹. The attack consists of adding a constant scalar value to every pixel, which can be interpreted as mostly a change in background colour. To better characterize the two models, we test beyond the limits of their threat model by including perturbations larger than 0.3. To do so, we disable the check in their script that verifies the attack data set has $\epsilon \leq 0.3$ w.r.t to the natural test set, but we still clip all values to the valid input range.

models converge to this configuration, and their respective values of the non-zero elements are (1.34, 0.86, 0.60) and (1.26, 0.80, 0.52). Kernels did have a more distributed representation in subsequent layers, but the pattern observed in the first layer was concerning. This is partly why we find one of the main recommendations made by Madry et al. (2018) to be problematic, namely that “*increasing capacity improves robustness*”, given that their models are choosing to not use the capacity they *already* have. Their justification is that more capacity is required to train with a stronger adversary such as PGD, but this contradicts earlier, more intuitive findings in Tanay & Griffin (2016), that a properly regularized “nearest centroid” classifier is unaffected by adversarial examples. We maintain that extraneous capacity is actually a *liability* in terms of robustness.

Although the models are reasonably well-behaved under their limited threat model, we maintain that increased sensitivity to a DC offset, as shown by the large shift down and to the left between the cyan filled area with dash-dot border, to orange area, is clearly undesirable. The right edge of each filled area plots accuracy when the offset is subtracted from the original images, while the left edge is when it is added.

4.2. Non-Example Gradient Ascent Attack

Rather than starting with correctly classified inputs and assessing how much accuracy is maintained after perturbing them by a finite amount, we can instead perform gradient ascent on random noise until the probability assigned to

¹https://github.com/madrylab/mnist_challenge
https://github.com/madrylab/cifar10_challenge

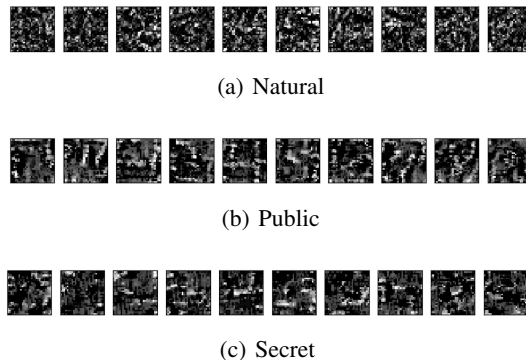


Figure 2. Non-examples classified with 100% confidence as each of the MNIST digits 0 through 9 (read from left to right) by the three models from Github¹. (a) is un-protected, while [(b) and (c)] are defended with 40 iterations of PGD in the inner-loop, up to $\epsilon_{\max} = 0.3$ and step size of 0.01. Some digits can almost be identified, such as a “3”, “4”, and “7” in (b).

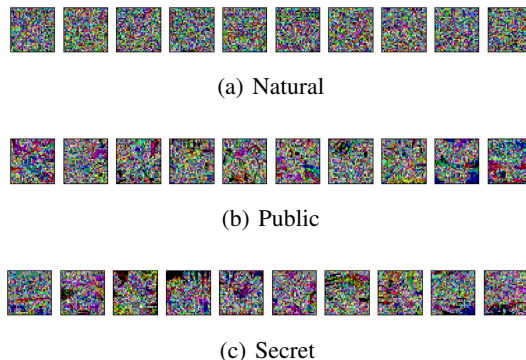


Figure 3. Non-examples classified with 100% confidence as each of the CIFAR-10 classes 0 through 9 (read from left to right) by the three state-of-the-art WideResNet (32 layers, width factor 10) models from Github¹. (a) is unprotected, while [(b) and (c)] are defended with 10 and 7 steps of PGD training respectively, with $\epsilon_{\max} = 8$ and a step size of 2.

a desired target class is maximized. Intuitively, a *robust* model should respond in one of two ways: the input could be classified with *low* confidence, since it is very distant from any natural example in the training distribution. Alternatively, if it is to be classified with high confidence, the noise should be meaningfully transformed into something that resembles a legitimate example. This is exactly the test that was performed by Nguyen et al. (2015), which found that state-of-the-art deep neural networks respond in neither of these two ways. These models consistently classify unrecognizable noise images as belonging to a natural object class with very high confidence (e.g 99.99%).

The attack consists of first sampling a noisy image $\mathcal{N}(0, 0.1) \in \mathbb{R}^{28 \times 28}$ for MNIST, and $\mathcal{N}(0, 0.1) \in \mathbb{R}^{32 \times 32 \times 3}$ for CIFAR-10. A numpy random seed of 0 was

used, along with 100 steps of gradient ascent on each of the target classes using a step size of 0.01. All images were clipped to the valid pixel range of $[0, 1]$ for MNIST and $[0, 255]$ for CIFAR-10. Identical per image standardization is used as in Madry et al. (2018). The second from right images in Figure 3 [(b) and (c)] corresponding to the “ship” class have more blue pixels for water near the corners, which is somewhat encouraging. Overall, the images are not nearly as convincing as those in subsequent sections where strong weight decay or low-precision is used.

5. Toy Experiments

Here, we establish intuition with toy problems that offer significant insight into the phenomenon of adversarial examples. We attempt to generalize observations made regarding these experiments to challenge claims made in the literature. These experiments provide a nice lens for subsequent discussions regarding higher-dimensional image classification problems and manifolds, such as with CIFAR-10 and ImageNet in subsequent sections.

5.1. Binary Classification

We first study MNIST three vs. seven classification, as it is a nearly linearly separable problem for which an optimal expert model is known a priori. By optimal, we mean a single set of parameters, θ , for a particular model architecture, that are best suited to a particular task, and confer good robustness. We do *not* mean that we achieve zero test error, as this practically *guarantees* that adversarial examples will exist (Gilmer et al., 2018). Zero-error implies that models with fixed capacity are forced to cheat, by memorizing peculiarities or surface statistics in the data that generalize in a narrow distributional sense (Jo & Bengio, 2017).

5.1.1. THREES VERSUS SEVENS

We wish to emphasize several points in reference to the weight visualization from Figure 4, and empirical results from Table 1.

Clean test accuracy was a weak measure of model fitness. For example, model 4(f), which had the highest test accuracy, was also the most vulnerable to attack. Adversarial training does not always help. In this case, it was desirable to be completely invariant to certain areas of the input corresponding to background pixels. Naive adversarial training implementations actually interfere with learning this optimal solution. Additionally, a model that was already well-tuned hardly benefited from adversarial training (e.g. compare 4(k) and 4(l)), and several undefended low-precision models with 5–8 bit representations outperformed the augmented full-precision one 4(l).

Very low-precision representations (e.g. below 4-bits) even-

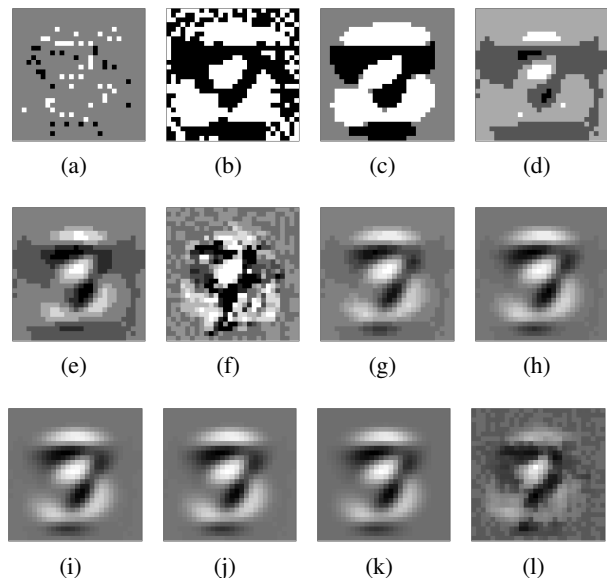


Figure 4. Depiction of a logistic regression model’s weights for various levels of quantization after training on an MNIST three vs. seven binary classification task. Models [(a)–(c)] are 1-bit, (d) is 2-bit, [(e) and (f)] are 3-bit, [(g), (h), (i), (j)] are 4, 5, 6, and 7-bits respectively, while [(k) and (l)] are 32-bit precision. All weights were initialized by subtracting the average seven from the average three, except for in (a) and (b). Models were finetuned for 50k steps by Adam using the sigmoid cross entropy loss, a batch size of 128, learning rate of $1e-5$, and L2 weight decay with a regularization constant of $5e-2$. Models (f) and (l) were trained with the same hyper-parameters, but on adversarial examples (Kurakin et al., 2017).

tually become a compromise in terms of accuracy on both the clean and perturbed test sets, as the number of parameters was already very low, and an insightful initialization scheme and training procedure were already known. Models with weights that were not given “expert initialization” were far more sensitive to the choice of hyper-parameters, such as the standard deviation of the truncated normal distribution that was used to initialize models trained from scratch. This suggests that the robustness of much higher capacity models will be even more sensitive to such hyper-parameters.

Some configurations, such as the pruned binary model 4(a), fared surprisingly well in light of the learned weight matrices. However, this model is likely more vulnerable to single pixel or other L_0 constrained attacks like the Jacobian Saliency Map Attack (Papernot et al., 2015). We must be careful when drawing conclusions from only one type of attack. Here we only reported against the L_∞ norm FGSM.

This simple experiment leads to some common sense observations about robustness, and how it can be obtained through visualization where possible and benefitting from strong human judgement when available. Adversarial training or

Table 1. Accuracy of the logistic regression models from Figure 4 on test set and adversarial examples generated by fast gradient (sign) method (Goodfellow et al., 2015) with $\epsilon = 0.1$. Models were given “expert initialization” except 4(a) and 4(b) which were initialized from a truncated normal with $\sigma = 0.1$.

MODEL	BITS	TEST	FGM	NOTE
4(A)	1	95.8	66.7	RAND INIT + PRUNE
4(B)	1	96.7	34.0	RAND INIT
4(C)	1	96.2	55.9	PRUNE
4(D)	2	94.7	52.2	
4(E)	3	95.8	73.8	
4(F)	3	97.0	18.8	ADV. TRAINING
4(G)	4	95.3	77.3	
4(H)	5	95.8	82.8	
4(I)	6	95.8	84.1	
4(J)	7	95.8	84.5	
N/A	8	95.8	84.8	
N/A	32	94.8	80.1	NO TRAINING
4(K)	32	95.0	81.1	
4(L)	32	96.7	82.3	ADV. TRAINING

data-augmentation is not the only way to confer robustness, and in fact, it can exacerbate the problem if applied to a poorly tuned model. We acknowledge that the fast gradient method is not the only measure of robustness, but it is convenient and exact for the linear model used here. We explore stronger iterative attacks in subsequent sections. This experiment helps us expand on the observation of Gilmer et al. (2018) that the capacity required to achieve *zero* error on a given dataset is significantly greater than that required to achieve very *low* error. In this experiment, driving a model with fixed architecture and capacity to zero error makes it brittle, therefore the definition of acceptably *low* error requires sound human judgement. For this architecture and dataset combination, we suggest aiming for no less than $\approx 5\%$ error to generalize well.

5.1.2. SPHERES

To gain further insight we reproduce the dataset and two hidden-layer MLP from Gilmer et al. (2018) in which adversarial examples can be found on the manifold of a synthetic n -sphere dataset. The task is to classify two n -dimensional concentric spheres with differing radii. We make the problem more challenging by training on a semi-sphere and testing on the full-sphere. We notice the 1-bit weight, 2-bit activation model retains a tighter shape than the full-precision equivalent, which begins to sag and expand where there is a lack of support.

The lack of direct feedback between the real-valued weight update and the thresholding done in the forward pass could be seen as a form of inertia. One way to interpret the result in Figure 5 is that the binary weights vote for the status-quo and avoid contorting their decision boundary into unusual shapes in the absence of strong evidence.

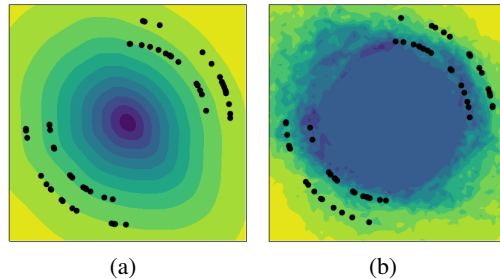


Figure 5. Depiction of decision boundary for MLPs trained on a variant of the 2-dimensional Spheres dataset from Gilmer et al. (2018), where we remove two opposing quadrants from the training set, but test on a full-sphere, a representation of higher-dimensional data sets that are inherently sparse. The full-precision MLP (a) flattens out in areas of the manifold that aren’t supported, whereas the 1-bit weight 2-bit activation MLP (b) retains a full-shape. Occam’s razor suggests that given a lack of evidence, it is desirable to preserve the simpler hypothesis (b) of “sphere” than a more complicated (a) “ellipse”. Best viewed in colour.

6. Non-Example Gradient Ascent Attack

We now show that reducing unexplored space through strong regularization mostly overcomes this limitation, such that unrecognizable images are in fact classified with *low* confidence. Furthermore, when we perform gradient ascent on an initial noise image, we obtain plausible legitimate images for each of the respective classes, without using a decoder or reconstruction objective of any kind.

Obtaining ground-truth calibrated confidence and uncertainty estimates for predictions made by deterministic models is somewhat of an open problem (Gal, 2016), but for comparison purposes we adopt the same procedure as in Nguyen et al. (2015), where confidence is measured as the magnitude of the largest softmax probability. This measure of confidence is fairly standard in the non-adversarial examples literature, and various “softmax smoothing” approaches have been proposed to make these estimates more reliable, such as temperature scaling (Guo et al., 2017) or penalizing high entropy distributions (Pereyra et al., 2017). The former approach is very similar to the defeated defensive distillation approach that similarly employed softmax temperature scaling (Papernot et al., 2016), providing a false sense of security (Carlini & Wagner, 2017).

For both Sections 6.1 and 6.2, we use the following vanilla three-layer convolutional network described by Table 2 with ReLU activations, and a linear softmax readout layer. Batch normalization (Ioffe & Szegedy, 2015) is only used with low-precision layers to ensure quantization is centered around zero.

Table 2. CNN architecture for experiments in Sections 6.1 and 6.2.

Layer	H	W	C_{in}	C_{out}	stride	padding
Conv1	8	8	img_{ch}	n_f	2	SAME
Conv2	6	6	n_f	$2 \times n_f$	1	VALID
Conv3	5	5	$2 \times n_f$	$2 \times n_f$	1	VALID

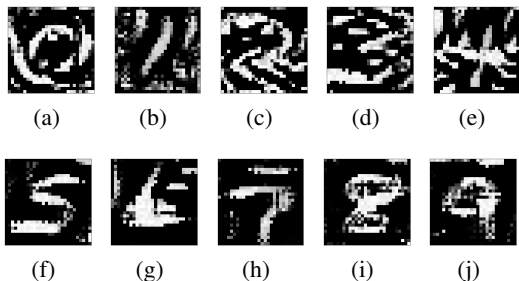


Figure 6. Generating MNIST examples with 1-bit (*top*) and full-precision (*bottom*) models after 100 iterations of gradient sign ascent on each target class with a step size of $1e-2$. An L_2 regularization constant of $\lambda = 0.5$ was used with the full-precision model and $\lambda = 0.05$ on the first layer of the 1-bit model which was retained in full-precision. Examples are classified with 45.6%–78.0% [(b) and (c)] for the 1-bit model, and 35.2%–52.2% [(h) and (i)].

6.1. Generating MNIST examples

We now attempt to explain why it is possible to generate such natural images without using a generative model. It was recently shown that adversarial examples for the MNIST dataset span an approximately 25 dimensional submanifold, which is mostly shared between models, thus enabling *attack transferability* (Tramèr et al., 2017). As we will see in comparison to ImageNet, this is a comparatively modest volume of unexplored example space to be eliminated. Further, MNIST classes are relatively densely sampled in the training set with respect to their low dimensionality, therefore strong L_2 weight decay is sufficient to compress the representation space. Interestingly, the binarized models seemed to always yield plausible pen strokes independent of other hyper-parameter settings, suggesting they could be a good starting point.

We emphasize that the images in Figure 6 were generated with an ordinary convolutional neural network, and that no decoder or reconstruction penalty is used to modify the normal training procedure in any way. All examples are classified with significantly less confidence than the unrecognizable *fooling images* from Nguyen et al. (2015).

6.2. Generating CIFAR-10 examples

In this section, we extend the same approach to the CIFAR-10 data set (Krizhevsky, 2009). To better contextualize

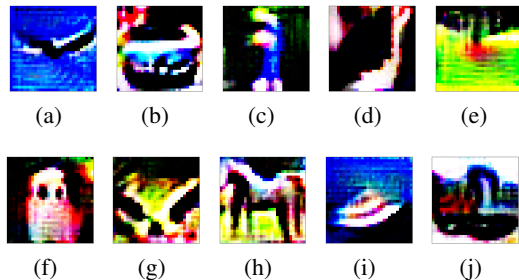


Figure 7. Generating CIFAR-10 examples with a full-precision discriminative model trained with 20 iterations of PGD (Madry et al., 2018) with $\epsilon = 0.3$, and 0.05 L_2 weight decay on first and last layers. Gradient ascent performed on a noisy image for 100 iterations with a step size of $1e-2$. Predictions are made with 28.6%–53.6% [(e) and (c)] confidence.



Figure 8. A visualization of all sixty-four ($n_f = 64$) 8×8 convolution filters from the first layer of our three-layer convolutional network trained on CIFAR-10 with 20 steps of PGD up to $\epsilon_{\max} = 0.3$ with an L_∞ norm. A regularization constant of 0.05 was used with L_2 weight decay. The model maintains 72% of its 56% clean test set accuracy when attacked with an $L_\infty - \epsilon_{\max} = 8/255 \approx 0.031$ constrained PGD adversary for 50 attack steps.

the images in Figure 7, compare with the equivalent noisy images that were classified with 100% confidence by “state-of-the-art” models from Madry et al. (2018) in Figure 3.

It is interesting to observe that the L_2 weight decay used with the model visualised in Figure 8 does not have the effect one might naively assume: to suppress the magnitude of the *average* element across *all* kernels, more or less equally. Instead, the weight decay objective is realized by dropping the majority of filters entirely ($\approx 72\%$), and focusing on primitive concepts. A dedicated filter for each of the pri-

Table 3. Single crop (224px) ResNet-18 error rates vs. FGSM perturbation amount for ImageNet misclassification attack for various settings of precision for weights (W), activations (A), and gradients (G). Attacks used 32-bit gradients to minimize *gradient masking*, regardless of the gradient precision used during training. ResNets were only trained for 76 epochs rather than the full 110 in Zhou et al. (2016) to reduce overfitting.

W,A,G	Error	Clean	eps=2	eps=4	eps=8
32,32,32	Top-1	38.8%	97.9%	98.8%	98.8%
	Top-5	16.2%	83.5%	88.7%	90.7%
3,3,32	Top-1	40.7%	97.8%	98.8%	98.9%
	Top-5	17.3%	83.1%	88.7%	90.7%
3,3,8	Top-1	40.2%	97.8%	98.7%	98.8%
	Top-5	17.2%	83.5%	89.0%	90.8%
3,3,6	Top-1	40.5%	97.6%	98.7%	98.7%
	Top-5	17.2%	82.8%	88.5%	90.7%
2,2,32	Top-1	45.4%	97.4%	98.5%	98.9%
	Top-5	20.4%	83.3%	88.9%	91.2%
2,2,6	Top-1	44.9%	97.5%	98.8%	98.9%
	Top-5	20.4%	83.3%	89.3%	91.3%
1,2,32	Top-1	50.4%	97.9%	98.8%	99.1%
	Top-5	24.8%	86.9%	91.8%	93.8%
1,2,8	Top-1	51.1%	97.8%	98.7%	98.8%
	Top-5	25.6%	86.7%	91.5%	93.1%
1,2,6	Top-1	50.2%	97.9%	98.9%	98.9%
	Top-5	24.8%	86.8%	91.8%	93.4%
1,1,32	Top-1	59.6%	96.8%	98.4%	98.9%
	Top-5	33.5%	86.4%	92.1%	94.2%
1,1,8	Top-1	59.6%	96.9%	98.5%	98.7%
	Top-5	33.5%	86.4%	92.0%	93.7%

mary colours (R, G, B) is learned, along with some vertical, diagonal, and horizontal edge detectors. We suspect this is a near-optimal strategy for a model of this architecture and capacity as these features clearly generalize to a broad class of naturally occurring images, while minimizing sensitivity along directions of low variance in the data. This is reflected by the excellent robustness of the model under a very strong PGD attack, and it retains a significantly higher percentage of its natural test accuracy than the state-of-the-art models defended with PGD. This model achieves just 5.6% under the state-of-the-art robustness of 45.8% for CIFAR-10 for the same PGD attack set on the WideResNet (W32-10) of Madry et al. (2018), despite having 31.7% less clean test accuracy and only 1.5% as many parameters. These results concur with overwhelming evidence that modern deep neural networks are over-parameterized, e.g see (Rosenfeld & Tsotsos, 2018).

6.3. ImageNet Classification

The data in Table 3 could be interpreted in one of two ways, either that ResNets are fragile to precision reduction, or that

they are prone to overfitting since their improvements on the natural test set consistently disappear compared to low-precision variants when *attacking* with various perturbation sizes. The latter argument implies that the incremental accuracy improvement of the full-precision model on the test set does not generalize. We also found that retraining the WideResNet from Madry et al. (2018) with one or two more orders of magnitude L_2 weight decay, but less than used with our vanilla CNN, fails to yield more than 30% test accuracy with otherwise identical hyper-parameters.

Although the error rates in Table 3 are high, none of the models were trained with data augmentation and *no* other defense for ImageNet currently exists that does much better than what we show here. The defense of Xie et al. (2018) consisting of a randomization input layer was found to achieve 0% accuracy by Athalye et al. (2018) for the same threat model (L_∞ and $\epsilon = 8$), although we acknowledge that a stronger iterative attack was used in that case. We suggest that starting with smaller models that can handle strong weight decay or precision reduction is worth exploring as a natural defense.

7. Discussion

It is important that we move away from data augmentation-based techniques for conferring robustness. In addition to slowing down training by a factor equal to the number of steps of gradient ascent per weight update, these techniques have significant limitations. Models defended this way are vulnerable to perturbations just a small distance beyond that used during training, which can be observed in Figure 2 of the (Madry et al., 2018) paper. As illustrated by Tanay & Griffin (2016), a prerequisite for generating high quality adversarial examples during training is a well regularized model, otherwise, the examples will lie extremely close to the decision boundary and sub-manifolds. As we showed, an attacker is likely to be able to find a different attack that works well on a model defended with a particular variant of adversarial training. Conversely, there is no reason to expect properly regularized models to suffer from these same limitations, as they fundamentally alter the geometry of the decision boundary, and maximize entropy in the unexplored representation space.

8. Conclusion

We have shown that small, regularized models, retain a high percentage of their natural test accuracy against adversarial examples. A promising direction for future research in robust machine learning, without relying on data augmentation, is to start small. Once it can be shown that meaningful features are learned, e.g., by testing that whatever little accuracy that is obtained does not degrade with local adversarial and global non-examples, then progressively add capacity in an iterative loop until satisfactory performance is reached.

ACKNOWLEDGMENTS

The authors wish to acknowledge the financial support of NSERC, CFI and CIFAR. The authors also acknowledge hardware support from NVIDIA and Compute Canada. We thank Brittany Reiche for editing and improving the readability of our manuscript.

References

- Athalye, Anish, Engstrom, Logan, Ilyas, Andrew, and Kwok, Kevin. Synthesizing Robust Adversarial Examples. *arXiv preprint arXiv:1707.07397*, July 2017. URL <http://arxiv.org/abs/1707.07397>.
- Athalye, Anish, Carlini, Nicholas, and Wagner, David. Obfuscated Gradients Give a False Sense of Security: Circumventing Defenses to Adversarial Examples. *arXiv preprint arXiv:1802.00420*, February 2018. URL <http://arxiv.org/abs/1802.00420>.
- Bau, David, Zhou, Bolei, Khosla, Aditya, Oliva, Aude, and Torralba, Antonio. Network dissection: Quantifying interpretability of deep visual representations. In *Computer Vision and Pattern Recognition*, 2017.
- Bengio, Yoshua, Léonard, Nicholas, and Courville, Aaron C. Estimating or propagating gradients through stochastic neurons for conditional computation. *CoRR*, abs/1308.3432, 2013. URL <http://arxiv.org/abs/1308.3432>.
- Buckman, Jacob, Roy, Aurko, Raffel, Colin, and Goodfellow, Ian. Thermometer encoding: One hot way to resist adversarial examples. *International Conference on Learning Representations*, 2018. URL <https://openreview.net/forum?id=S18Su--CW>.
- Carlini, Nicholas and Wagner, David A. Defensive distillation is not robust to adversarial examples. *arXiv preprint arXiv:1607.04311*, 2017.
- Cisse, Moustapha, Bojanowski, Piotr, Grave, Edouard, Dauphin, Yann, and Usunier, Nicolas. Parseval networks: Improving robustness to adversarial examples. In Precup, Doina and Teh, Yee Whye (eds.), *Proceedings of the 34th International Conference on Machine Learning*, volume 70 of *Proceedings of Machine Learning Research*, pp. 854–863, International Convention Centre, Sydney, Australia, 06–11 Aug 2017. PMLR.
- Courbariaux, Matthieu and Bengio, Yoshua. Binarynet: Training deep neural networks with weights and activations constrained to +1 or -1. *arXiv preprint arXiv:1602.02830*, 2016.
- Dhillon, Guneet S., Azizzadenesheli, Kamyar, Bernstein, Jeremy D., Kossaifi, Jean, Khanna, Aran, Lipton, Zachary C., and Anandkumar, Animashree. Stochastic activation pruning for robust adversarial defense. *International Conference on Learning Representations*, 2018. URL <https://openreview.net/forum?id=H1uR4GZRZ>.
- Dube, Simant. High dimensional spaces, deep learning and adversarial examples. *arXiv preprint arXiv:1801.00634*, 2018.
- Fawzi, Alhussein, Fawzi, Omar, and Frossard, Pascal. Analysis of classifiers’ robustness to adversarial perturbations. *arXiv preprint arXiv:1502.02590*, 2015.
- Gal, Yarin. *Uncertainty in Deep Learning*. PhD thesis, University of Cambridge, 2016.
- Galloway, Angus, Taylor, Graham W., and Moussa, Medhat. Attacking binarized neural networks. *International Conference on Learning Representations*, 2018. URL <https://openreview.net/forum?id=HkTEFfZRb>.
- Gilmer, Justin, Metz, Luke, Faghri, Fartash, Schoenholz, Samuel S., Raghu, Maithra, Wattenberg, Martin, and Goodfellow, Ian. Adversarial Spheres. *arXiv preprint arXiv:1801.02774*, January 2018. URL <http://arxiv.org/abs/1801.02774>.
- Goodfellow, Ian. J., Shlens, Jonathon., and Szegedy, Christian. Explaining and Harnessing Adversarial Examples. *Proceedings of the International Conference on Learning Representations*, 2015.
- Gu, Shixiang and Rigazio, Luca. Towards deep neural network architectures robust to adversarial examples. *ICLR Workshop*, 2015.
- Guo, Chuan, Pleiss, Geoff, Sun, Yu, and Weinberger, Kilian Q. On calibration of modern neural networks. In *Proceedings of the 34th International Conference on Machine Learning, ICML 2017, Sydney, NSW, Australia, 6-11 August 2017*, pp. 1321–1330, 2017. URL <http://proceedings.mlr.press/v70/guo17a.html>.
- Guo, Chuan, Rana, Mayank, Cisse, Moustapha, and van der Maaten, Laurens. Countering adversarial images using input transformations. *International Conference on Learning Representations*, 2018. URL <https://openreview.net/forum?id=SyJ7ClWCb>.
- Ioffe, Sergey and Szegedy, Christian. Batch normalization: Accelerating deep network training by reducing internal covariate shift. *ICML*, 2015.
- Jo, Jason and Bengio, Yoshua. Measuring the tendency of cnns to learn surface statistical regularities. *arXiv preprint arXiv:1711.11561*, 2017.

- Krizhevsky, Alex. Learning multiple layers of features from tiny images. Technical report, 2009.
- Kurakin, Alexey, Goodfellow, Ian J., and Bengio, Samy. Adversarial machine learning at scale. *Proceedings of the International Conference on Learning Representations*, 2017.
- Madry, Aleksander, Makelov, Aleksandar, Schmidt, Ludwig, Tsipras, Dimitris, and Vladu, Adrian. Towards deep learning models resistant to adversarial attacks. *International Conference on Learning Representations*, 2018. URL <https://openreview.net/forum?id=rJzIBfZAb>.
- Nguyen, Anh, Yosinski, Jason, and Clune, Jeff. Deep neural networks are easily fooled: High confidence predictions for unrecognizable images. In *CVPR*, pp. 427–436. IEEE Computer Society, 2015.
- Papernot, N., McDaniel, P., Wu, X., Jha, S., and Swami, A. Distillation as a defense to adversarial perturbations against deep neural networks. In *2016 IEEE Symposium on Security and Privacy (SP)*, pp. 582–597, May 2016. doi: 10.1109/SP.2016.41.
- Papernot, Nicolas, McDaniel, Patrick D., Jha, Somesh, Fredrikson, Matt, Celik, Z. Berkay, and Swami, Ananthram. The limitations of deep learning in adversarial settings. [abs/1511.07528](https://arxiv.org/abs/1511.07528), 2015. URL <http://arxiv.org/abs/1511.07528>.
- Pereyra, Gabriel, Tucker, George, Chorowski, Jan, Kaiser, Lukasz, and Hinton, Geoffrey E. Regularizing neural networks by penalizing confident output distributions. *ICLR Workshop*, 2017.
- Rosenfeld, Amir and Tsotsos, John K. Intriguing properties of randomly weighted networks: Generalizing while learning next to nothing. *International Conference on Learning Representations*, 2018. URL <https://openreview.net/forum?id=Hy-w-2PSf>. Under review for the workshop track.
- Samangouei, Pouya, Kabkab, Maya, and Chellappa, Rama. Defense-GAN: Protecting classifiers against adversarial attacks using generative models. *International Conference on Learning Representations*, 2018. URL <https://openreview.net/forum?id=BkJ3ibb0->.
- Song, Yang, Kim, Taesup, Nowozin, Sebastian, Ermon, Stefano, and Kushman, Nate. Pixeldefend: Leveraging generative models to understand and defend against adversarial examples. *International Conference on Learning Representations*, 2018. URL <https://openreview.net/forum?id=rJUYGxbCW>.
- Szegedy, Christian, Zaremba, Wojciech, Sutskever, Ilya, Bruna, Joan, Erhan, Dumitru, Goodfellow, Ian, and Fergus, Rob. Intriguing properties of neural networks. *Proceedings of the International Conference on Learning Representations*, 2014.
- Tanay, Thomas and Griffin, Lewis D. A boundary tilting perspective on the phenomenon of adversarial examples. *arXiv preprint arXiv:1608.07690*, 2016.
- Tramèr, Florian, Papernot, Nicolas, Goodfellow, Ian, Boneh, Dan, and McDaniel, Patrick. The space of transferable adversarial examples. *arXiv preprint arXiv:1704.03453*, 2017.
- Xie, Cihang, Wang, Jianyu, Zhang, Zhishuai, Ren, Zhou, and Yuille, Alan. Mitigating adversarial effects through randomization. *International Conference on Learning Representations*, 2018. URL <https://openreview.net/forum?id=Sk9yuql0Z>.
- Zhou, Shuchang, Wu, Yuxin, Ni, Zekun, Zhou, Xinyu, Wen, He, and Zou, Yuheng. Dorefa-net: Training low bitwidth convolutional neural networks with low bitwidth gradients. *arXiv preprint arXiv:1606.06160*, 2016.